2011

Measurement of Particle Size Distribution in a Swine Building

Sheryll B. Jerez
Stephen F Austin State University, jerezs@sfasu.edu

Yuanhui Zhang
University of Illinois at Urbana-Champaign

X Wang

MEASUREMENT OF PARTICLE SIZE DISTRIBUTION IN A SWINE BUILDING

S. B. Jerez, Y. Zhang, X. Wang

ABSTRACT. *The majority of the research in animal buildings has been on measured concentrations of contaminants that the workers and animals are exposed to; emission measurements have only gained attention in recent years due to potential federal regulations on air quality emissions from animal feeding operations (AFOs). The contribution of AFOs to ambient PM_{10} and $PM_{2.5}$ entails reliable measurement of particle size distribution. The objective of this study was to measure and compare the size distribution of particulate matter (PM) at multiple locations inside and at the exhausts of a wean-to-finish commercial swine building. The particle size distribution was measured by collecting total suspended particulate matter on Teflon filters and using Coulter Counter and Horiba LA-300 analyzers for particle size distribution analyses. Results showed that the mass median diameter (MMD) of swine PM at the exhaust was about 14% lower than the average MMD indoors (26.84 vs. 31.55 μm), while the geometric standard deviations were about the same (1.85 vs. 1.86). In addition, the average percentage by volume of PM_{10} indoors was about 8%, while the percentage of PM_{10} leaving the building was 10%. In terms of the mass concentrations, PM_{10} indoors ranged from 0.014 to 0.125 mg m^{-3}, while at the exhaust PM_{10} ranged from 0.02 to 0.15 mg m^{-3}. This study will aid in understanding the exposure of workers to particles indoors and in quantifying the contribution of a commercial swine building to emissions of PM_{10} in the atmosphere.*

Keywords. *Air quality, Animal housing, Coulters, Dust, Emissions, Particle size, Particles, Swine.*

Although the number of animal farms in the U.S. has declined since reaching its peak in 1935 of about 6.5 million, the annual production of livestock and animal products has risen steadily over the last century (NAS, 2003) due to the increased farm size and the number of animals born and raised per farm. The expansion of intensive livestock production systems leads to public concern about the associated environmental and health issues. These issues include the contribution of air emissions from confined animal buildings to ambient air pollution and the possible public health effects.

The majority of the research in animal buildings has been on measured concentrations of contaminants that the workers and animals are exposed to. Thus, it is well-established knowledge that the levels of pollutants, particularly PM, in animal buildings are influenced by animal category (e.g., poultry or swine), animal activity, bedding materials, and season, among others (Ellen at al., 2000; Predicala et al., 2001; O'Shaughnessy et al., 2002). In recent years, however, emission rate measurements of various pollutants from animal buildings have received considerable attention (Heber et al., 2001; Redwine and Lacey, 2001; Ni et al., 2000, 2002; Predicala and Maghirang, 2002; Gay et al., 2003; Jacobson et al., 2003; Jerez et al., 2005) due to increasing calls for federal air quality regulations regarding animal feeding operations (AFOs), which includes animal buildings. However, the existing emission data on AFOs are still insufficient, and there are substantial variations in the methods used for estimating emissions (NAS, 2003). Thus, in 2005, the U.S. Environmental Protection Agency (EPA) announced the Air Quality Compliance Agreement for AFOs that gave farmers an opportunity to participate in farm air emission studies. Monitoring in 24 sites was completed in 2009, and the final report is scheduled to be completed in 2011. The data will be used by the EPA, in part, to establish standard methodologies for monitoring emissions from AFOs.

From the regulatory standpoint, being able to quantify the contribution of particulate matter (PM) emission from AFOs to ambient PM_{10} and $PM_{2.5}$, which are being regulated by the EPA, entails accurate measurements of the particle size distribution (PSD) of PM emissions. Even though the standards call for direct measurements of the concentrations of the representative PM in AFOs, indirect determination of $PM_{2.5}$ and PM_{10} from the PSD is still considered a reliable alternative, especially when size-selective samplers are not readily available. Currently, there are a very limited number of PSD measurements in animal buildings (Vinzents, 1994; Sweeten et al., 1998; Predicala, et al., 2001; Schneider et al., 2001; Zhang et al, 2001; Capareda et al., 2005), and this study will contribute to this still limited body of literature.

The PSD instruments that have been used in animal building applications are the cascade impactor (Vinzents, 1994; Predicala et al., 2001), optical particle counter (OPC)

Submitted for review in August 2010 as manuscript number SE 8755; approved for publication by the Structures & Environment Division of ASABE in May 2011. Presented at the 2009 ASABE Annual Meeting as Paper No. 096565.

The authors are **Sheryll B. Jerez, ASABE Member Engineer,** Assistant Professor, College of Forestry and Agriculture, Stephen F. Austin State University, Nacogdoches, Texas; **Yuanhui Zhang, ASABE Member Engineer,** Professor, and **Xinlei Wang, ASABE Member Engineer,** Associate Professor, Department of Agricultural and Biological Engineering, University of Illinois at Urbana-Champaign, Urbana, Illinois. **Corresponding author:** Sheryll B. Jerez, College of Forestry and Agriculture, Stephen F. Austin State University, 419 E College at Raquet St., Nacogdoches, TX 75962; phone: 936-468-6614; e-mail: jerezs@sfasu.edu.

  ISSN 2151-0032

(Schneider et al., 2001), aerodynamic particle sizer (APS) (Zhang et al., 2001), and Coulter Counter (Sweeten et al., 1998; Capareda et al., 2005). These instruments (except the Coulter Counter, which is used in laboratories to analyze PM samples collected on filters) have to be exposed to the hostile environments of animal production facilities and are not meant to measure large particles. The operation of each PSD instrument is governed by one of the following principles: inertial classification, light scattering, or electrical sensing. This research collected total suspended particulate matter (TSP) on Teflon filters and used a Horiba LA-300 light scattering PSD analyzer and Coulter Counter to determine the PSD. The objectives of this research were to measure and compare the PSDs of PM sampled inside and at the exhaust of a swine building, and to compare the possible seasonal variation in PSD.

METHODS

FACILITY AND PM SAMPLING SYSTEMS

The research was carried out at a commercial swine facility located in McLean, Illinois. The facility had nine wean-to-finish buildings with a total capacity of 12,000 head. Measurements were conducted in one of the buildings containing 2300 (December 2005) to 2400 pigs (June 2006). Pigs were brought in when they were about three weeks old, weighing about 5 kg, and they were fed until they reached a market weight of about 115 kg. The entire production period took about 24 weeks, with the first 8 to 10 weeks for nursery and the next 16 weeks for raising the pigs to market weight.

The building was 64.6 m long, 12.2 m wide, and 4.6 m high. It had forty 3.3 × 5.7 m pens with a completely slatted floor underneath. The pens, which held 30 to 50 pigs each, were in two rows with 20 pens in each row. As shown in figure 1, the building had a 2.4 m deep pit underneath the floor where manure was stored for approximately one year and then land applied using a drag hose system. Two pens shared two tube-type feeders with an automatic feeding mechanism to control the amount of feed. Feed was released into a metal trough that also held water. Sows were fed twice daily, at around 6:00 a.m. and 2:30 p.m.

The building was mechanically ventilated with five-stage exhaust fans consisting of one variable-speed 91 cm fan and four single-speed 122 cm fans. It also had four single-speed and continuously running 46 cm pit fans. All fans had discharge diffuser cones and gravity-controlled shutters. The building was tunnel-ventilated during the sampling in June, with air drawn through electronically controlled curtains in an end wall opposite the exhaust fans (fig. 2). During mild weather, partial ventilation was also provided by the ceiling inlets. During the sampling in December, the building was ventilated solely through the 13 baffle-type ceiling inlets installed over the central walk alley (fig. 1); each inlet was

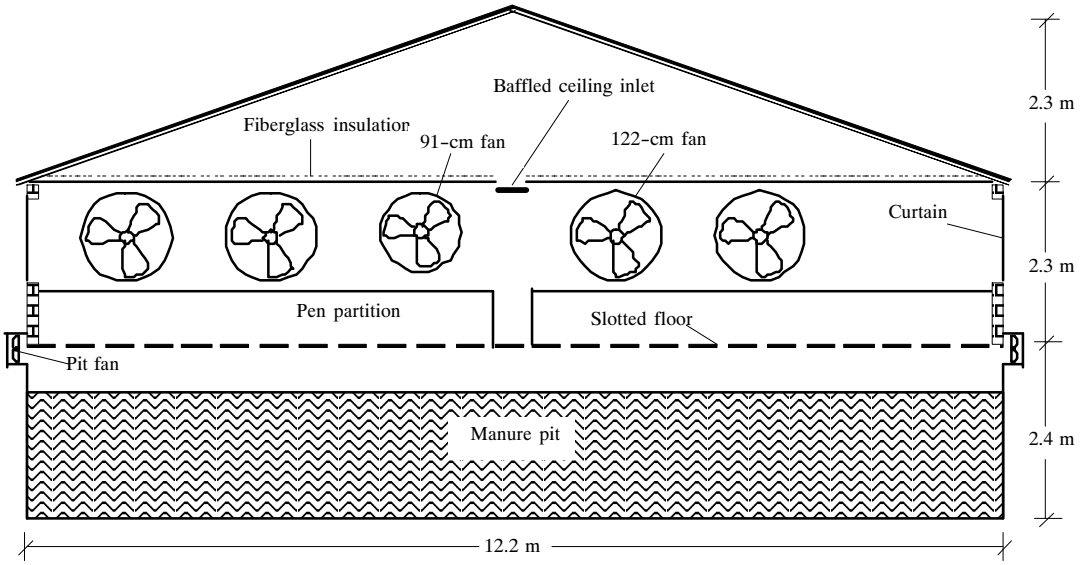

Figure 1. Schematic of the cross-section of the swine building.

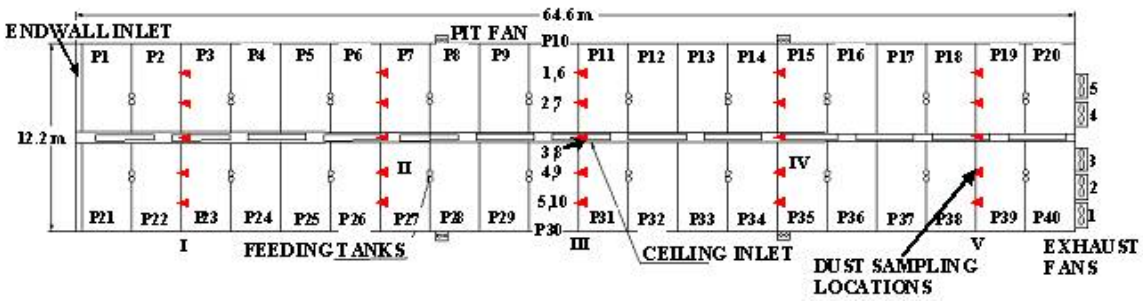

Figure 2. Plan view showing the sampling locations for TSP. P1 to P40 = pens 1 to 40. Roman numerals I to V refer to the cross-sectional planes. PM sampling locations 1 to 5 are 1.6 m above the floor; locations 6 to 10 are 0.8 m above the floor.

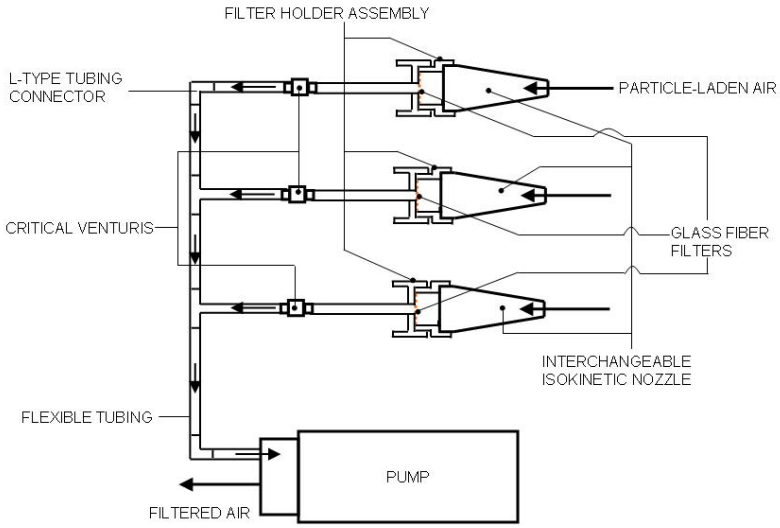

Figure 3. Schematic and components of the UIUC-TSP isokinetic sampler.

240 cm long and 40 cm wide. The building also had sidewall curtains that are manually opened when power interruptions occur to prevent buildup of heat, moisture, and contaminants inside the building.

Figure 2 is a plan view of the building showing the indoor TSP sampling locations. The mass concentrations of TSP were measured at 50 points located on five cross-sectional planes in the building (I, II, III, IV, and V in fig. 2). The cross-sectional planes were about 13 m apart. There were ten sampling locations on each cross-sectional plane. Five samplers were placed at about 1.6 m above the floor, and five were placed at about 0.8 m above the floor. For the indoor PSD measurements, only 18 samples from planes I, III, and V were analyzed. The mass concentrations at the 50 indoor locations were measured using five multipoint sampling systems made of CPVC pipe; each system consisted of a 10-point measuring array.

Each sampler in the array consisted of a 37 mm open-face filter holder (SKC, Inc., Eight Four, Pa.) and a critical venturi; all ten samplers in each array were connected to a 746 W sampling pump (model 1423-103Q-G625, Gast Manufacturing, Inc., Benton Harbor, Mich.). The open-face filter holder served both as the inlet and the filter holder. The samplers were oriented horizontally with the inlet facing toward the endwall inlet. With this orientation, the primary airflow during the measurements was about parallel to the filter plane, minimizing the effect of differing degrees of non-isokinetic sampling. The average air velocities at the 50 sampling locations were measured with a hot-wire anemometer (model 8340, TSI, Inc., St. Paul, Minn.) and ranged from 38 to 122 cm s^{-1} in June. In December, the air velocities were close to zero and below the measurement range of the anemometer. The critical-flow venturi was downstream of the filter and controlled the flow rate through the filter at 0.022 ±0.0002 m^3 min^{-1} (21.85 ±0.20 L min^{-1}) at a critical pressure of 10.21 ±0.90 kPa; the values represent averages and corresponding standard deviations.

The mass concentration of the TSP leaving the building through the exhaust fans was measured upstream of the fans using the UIUC-TSP isokinetic sampler shown in figure 3 (Jerez et al., 2006). It consisted of an isokinetic sampling head attached to a 37 mm open-faced filter holder, a critical venturi, and a sampling pump. The filters that were used for were either glass fiber (1.6 μm porosity, Whatman Type GF/A) or Teflon (2 μm porosity, Zefluor PTFE membrane). The sampling head was replaceable, i.e., different-size sampling heads can be used depending on the prevailing airflow velocity in the area. A sampling head with an entrance diameter of 14.6 mm, for a 2 m s^{-1} sampling velocity, was used. The nozzle was stainless steel with a 15° tapered edge and a cone angle of 6°; these values meet EPA's nozzle design specifications in Method 201A (EPA, 2000). Three sets of sampling head assemblies were connected to a sampling pump, allowing PM concentration to be measured at three locations across the cross-section of the exhaust fan. One nozzle was located in the middle section of the fan cross-section, and the other two were positioned at about 11 to 15 cm from the top and bottom outer edges of the fan. Isokinetic sampling was achieved by positioning the nozzles upstream of the two 122 cm exhaust fans facing the airflow at locations with an average velocity of 2 m s^{-1} ±10%. The velocity at the sampler locations was checked before and after sampling using a hot-wire anemometer (model 8340, TSI, Inc., St. Paul, Minn.).

Mass Concentration and Particle Size Distribution Measurements

The mass concentration of the TSP was measured by collecting PM onto either glass fiber (1.6 μm porosity, Whatman Type GF/A) or Teflon (2 μm porosity, Zefluor PTFE membrane) filters at an average flow rate of 0.02 m^3 min^{-1}. Glass fiber filters were used solely for mass concentration measurements, while Teflon filters were used for both mass concentration and PSD measurements. Prior to and after PM collection, the filters were conditioned in a dessicator with a constant temperature of 20°C ±2°C and a relative humidity of 15% ±5% for at least 24 h. The filters were weighed before and after sampling with a high-precision analytical balance (readability of 0.01 mg; model AG245, Mettler Toledo, Greifensee, Switzerland). The critical venturis were also calibrated prior to use with an automated venturi calibrator. The calibrator consisted of an accurate flow-metering device (Drycal BIOS model DC-2M, BIOS International, Butler, N.J.), a pump, a pressure control

unit, and a personal computer. The actual flow rates through the venturis when installed in the sampling setup in the farm were also measured using the Drycal BIOS.

The size distribution of PM was measured by collecting TSP on Teflon filters (2 μm porosity, Zefluor PTFE membrane). Eighteen samples indoors and six samples at the exhaust were collected at daytime and nighttime sampling events for five sampling days; each event lasted approximately 12 h. The indoor samples were collected from sampling locations 1, 3, 5, 6, 8, and 10 at planes I, III, and V in figure 2. Exhaust samples were collected upstream of fans 2 and 5 in figure 2. A Coulter Counter (Multisizer III, Beckman Coulter Inc., Fullerton, Cal.) and Horiba LA-300 light scattering PSD analyzer (Horiba, Ltd., Kyoto, Japan) were used for PSD analyses. The Coulter Counter was used for the samples collected in December, and the analyses were done in the Department of Biological and Agricultural Engineering at Texas A&M University. The Horiba LA-300 was used for the samples collected in June due to its availability in the Department of Agricultural and Biological Engineering at UIUC. In order to minimize the loss of samples, the inlet section of each sampler was reassembled and the inlet and outlet ports were sealed with plugs prior to transport to the laboratory for analysis. All samplers were also placed in sealed containers in an upright position during transport.

The Coulter Counter measures the number and size of particles suspended in an electrolyte using the electrical sensing zone method. The particles, suspended in a weak electrolyte solution, are drawn through a small aperture having an immersed electrode on either side. An aperture of 100 μm, which allowed particles with diameters of 2.95 to 60 μm to be measured, was used in the analysis. The voltage applied across the aperture creates the sensing zone. As each particle passes through the aperture (voltage zone), it displaces its own volume of conducting liquid, momentarily increasing the impedance of the aperture. This change in impedance produces a tiny but proportional current flow into an amplifier that converts the current fluctuations into a voltage pulse large enough to be measured accurately. The amplitude of this pulse is proportional to the volume of the particle that produced it. The pulses generated by the particles are counted and the pulse height is analyzed to determine the number of particles and particle volume, respectively. The pulse data are then stored to up to 300 channels (user-defined and depends on the instrument) (Beckman Coulter, 2000). Results from the Coulter Counter analysis were in the form of equivalent spherical diameter (ESD) versus the distribution based on elapsed time, particle count, and precise volumes. Since most particles are irregularly shaped, the volumetric response is invaluable, as volume is the only single measurement that can be made of an irregular particle to characterize its size (Lines, 1991). In air quality applications, volume measurement is often converted to equivalent volumetric diameter.

The Horiba LA-300 light scattering PSD analyzer (Horiba, Ltd., Kyoto, Japan) uses the interaction between the particles and light in measuring PSD. It applies the Mie scattering theory and relates the intensity distribution of the scattered light with the PSD (Horiba, 2001). The resulting PSD can be based on length, number, area, or volume. In this analysis, volume-based PSD was used. This instrument had an operating size range of 0.1 to 600 μm. The Teflon filter containing the collected PM was placed in a beaker containing approximately 20 mL of pre-filtered 5% lithium chloride-methanol solution. The particles were dispersed in the solution by exposing the filter to an ultrasonic bath for 15 min; this length of time has been established by Texas A&M as appropriate to remove almost all of the particles from the filter without damaging the particles (Buser, 2004). The dispersed solution was then added to the pre-filtered dispersant in the sample chamber. The concentration of the particles in the sample chamber, expressed as transmittance, was maintained between 75% and 90% for about 92% of the samples analyzed. The remaining 8% of the samples were too diluted but could still be reliably analyzed at concentrations between 90% and 95%. Each sample was analyzed three times by circulating the solution already contained in the sample chamber back to the flow cell two more times after completing the first analysis.

Measurement of Ventilation Rate and Outside Air Temperature

The ventilation rate in the building was monitored continuously using impeller anemometers installed downstream of the fans but inside the fan cones. Each anemometer measured the total flow rate through a fan by measuring the air speed near the center and consisted of an 18 cm diameter vane attached to a sealed-bearing direct current (DC) generator that produced a 0 to 1 VDC output proportional to the rotational speed. Prior to using the anemometers, they were calibrated in the fan test chamber in the Bioenvironmental Engineering Structure Systems (BESS) lab at the University of Illinois at Urbana-Champaign. The fan test chamber was designed according to ASHRAE 51-1985/AMCA 210-1985 and was capable of measuring airflow from 0.4 to 13 m s^{-1}. The specific location of the anemometer *in situ* was predetermined during the calibration in the laboratory.

The temperature outside the building was monitored every 60 s at five sampling locations using copper-constantan thermocouples (type T) connected to a datalogger (model CR23X, Campbell Scientific, Inc., Logan, Utah). This type of thermocouple has a measurement range of 0°C to 370°C, an accuracy of 1°C or ±0.75%, and a response time of 15 s. The thermocouples were calibrated prior to use at a measurement range of 0°C to 40°C using a dry block calibrator (model PB-35L, Techne (Cambridge) Limited, N.J.) and a CR23X datalogger. The calibration equation for each thermocouple was obtained by comparing the actual temperature reading of the thermocouple to that of the set temperature in the block calibrator.

Preliminary Experiments

Prior to sample analyses, the effects of the length of circulation and ultrasonic time on the PSD were first determined. In these preliminary analyses, approximately 30 mg of swine PM was dispersed in the 5% lithium chloride-methanol solution. The solution was then added to the pre-filtered dispersant in the sample chamber. Six PSD measurements were taken at six different times: 5, 10, 15, 30, 60, 120 min. Two more 30 mg samples were analyzed using the same procedure. The PSD values of the three samples were combined, and the average values were used in plotting the distributions. Results of a paired t-test analysis using SAS

showed that the PSDs measured at different times did not vary significantly ($p > 0.05$).

The effect of ultrasonic time on the measured PSD was also determined by dispersing four 30 mg samples of swine PM in about 20 mL of 5% lithium chloride-methanol solution for 10, 15, 20, and 30 min. The solution was then added to pre-filtered dispersant in the sample chamber. The same procedure was repeated two more times. The effect of ultrasonic time was only significant for particle diameters between 3 and 5 μm. The percentages by volume of particles up to 5 μm was significantly higher after 30 min than after 10 min, which could indicate break up of particles. For particles larger than 5 μm, the length of ultrasonic time did not affect their percentages by volume. Results of the analysis of variance in SAS showed that the difference between 15 and 30 min of ultrasonic time was not significant, indicating that 15 min of ultrasonic time is sufficient.

The choice of index of refraction is critical in calculating the PSD using the Horiba analyzer. The index of refraction of PM from animal buildings is still unknown, and estimating it is difficult since it consists of several components. Thus, it was measured using an ellipsometer available at the Material Research Laboratory (MRL) of the University of Illinois at Urbana-Champaign. The ellipsometer consisted of a He/Ne laser, a polarizer, an analyzer, and a detector. The ellipsometer at the MRL was fitted with a triangular glass cuvette to measure the index of refraction of the solution. The laser emitted electromagnetic radiation that was linearly polarized by the polarizer. The beam then struck the sample; some of the light was reflected and some passed into the sample contained in the cuvette. The light that entered the material at an angle did not continue in the same direction but was refracted to a different angle. The angle of refraction was measured by the ellipsometer and was used to calculate the index of refraction (Tompkins, 2006). Indices of refraction of different concentrations (7.4, 14.4, and 21.4 mg) of swine PM in 5% lithium chloride-methanol solution were measured, and the average value of 1.34 was used in the PSD analysis.

Data Analyses

The amount of PM collected on the filter was the difference between the weight of the loaded filter and its clean weight before sampling. The PM concentration was the mass of PM collected divided by the total volume of the sampled air. The total volume of sampled air was the product of the flow rate of the venturi and the total sampling time. Field blanks (filters enclosed in filter holders that were exposed to all aspects of sampling except collection) were also collected during sampling to measure incidental or accidental sample contamination during the whole process (sampling, transport, sample preparation, and analysis). The average amount of PM collected from the field blanks was subtracted from the collected PM mass. The mass of PM collected on the field blanks ranged from 0.00 to 0.10 mg.

As previously stated, the PSD values obtained by the Coulter Counter and Horiba LA-300 analyzers were based on equivalent spherical diameter (ESD) or d_e. ESD is the diameter of a sphere that would have the same volume and density as the particle. In order to convert the resulting PSD values to PM mass (volume) percent versus aerodynamic diameter (d_a), equations 1 and 2 (Zhang, 2005) were used:

$$d_a = \frac{1}{2}\left[\left(6.35\lambda^2 + 4d_p^2 C_c \frac{\rho_p}{\rho_o \chi}\right)^{\frac{1}{2}} - 2.52\lambda\right] \quad (1)$$

(for non-spherical particles, 0.1 μm < d_e < 3 μm)

$$d_a = d_p\left(\frac{\rho_p}{\rho_o \chi}\right)^{1/2} \quad (2)$$

(for non-spherical particles, $d_e \geq 3$ μm)

where ρ_o is the standard density of the particles (equal to 1000 kg m^{-3}), and χ is the dynamic shape factor ($\chi \geq 1$), with spherical particle having a dynamic shape factor of 1. Since there are currently no estimates for shape factor of animal PM, a shape factor of 1 was used in the calculations. Thus, equations 1 and 2 become:

$$d_a = \frac{1}{2}\left[\left(6.35\lambda^2 + 4d_e^2 C_c \frac{\rho_p}{\rho_o}\right)^{\frac{1}{2}} - 2.52\lambda\right] \quad (3)$$

(for spherical particles, 0.1 μm < d_e < 3 μm)

$$d_a = d_e\left(\frac{\rho_p}{\rho_o}\right)^{1/2} \quad (4)$$

(for spherical particles, $d_e \geq 3$ μm)

where C_c is the slip correction factor for particle diameter d_p or d_e (calculated using eq. 5), d_p is the actual geometric diameter of the particle, ρ_p is the particle density (measured with a pycnometer as 1450 kg m^{-3}), and λ is the mean free path of the carrying fluid. For air at standard conditions (pressure is 101.325 kPa and temperature is 20°C), λ is equal to 0.066 μm.

$$C_c = 1 + \frac{2.52\lambda}{d_p} \text{ (for } d_p \geq 0.1 \text{ μm)} \quad (5)$$

The lognormal distribution was used in the PSD analysis. Hinds (1999) indicated that lognormal distribution is the most common distribution used for characterizing particle sizes of aerosols. According to Zhang (2005), this distribution is particularly more widely used for particle populations coming from single sources. Lognormal distribution (Hinds, 1999; Cooper, 2001; Zhang, 2005) is the distribution that results when the distribution of the logarithm of particle size, $\ln(d_p/d_o)$, is Gaussian or normal; the reference size d_o is usually 1 μm. As shown in figure 4, when the mass fraction was plotted against the logarithmic scale of the particle size, the resulting distribution is approximately normal. The volume or mass distribution function was expressed as (Zhang, 2005):

$$df = \frac{1}{d_p \ln \sigma_g \sqrt{2\pi}} \times \exp\left(-\frac{(\ln d_p - \ln \text{MMD})^2}{2(\ln \sigma_g)^2}\right) d(d_p) \quad (6)$$

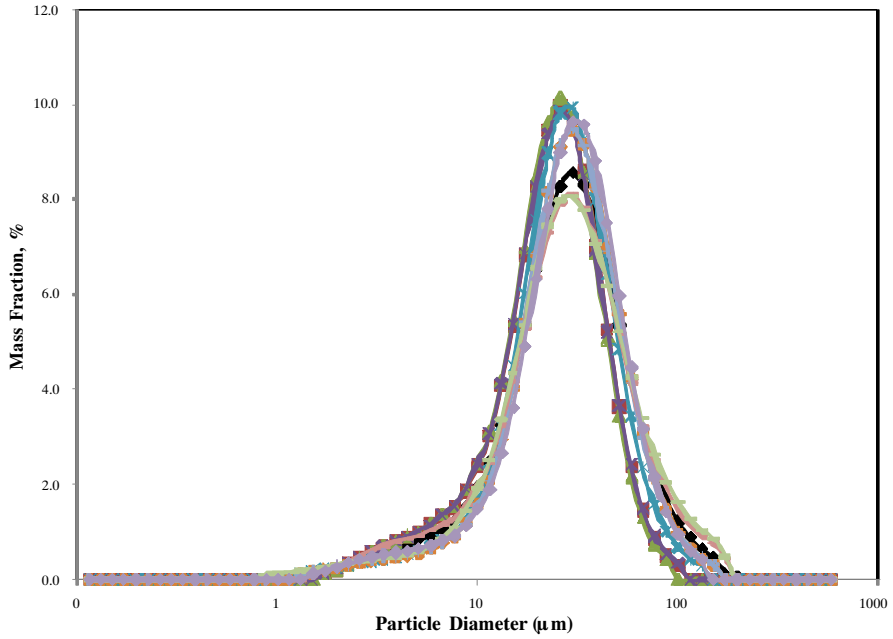

Figure 4. When the mass fraction was plotted against the log scale of the particle size, the typical distributions appear to be normally distributed. The data presented were taken from ten separate PSD measurements using the Horiba analyzer.

where MMD is the mass median diameter, or the diameter of the particle for which half of the total mass is larger and the other half is smaller. MMD was directly obtained from the cumulative distribution of the percentages of the particles by volume. The geometric standard deviation (σ_g, or GSD) is the ratio of the particle size associated with a cumulative mass of 84.1% and the median size (a cumulative mass of 50%), or between the 50% cumulative mass and the 15.9% cumulative mass, as presented in equation 7:

$$\sigma_g = \frac{d_{84.1\%}}{d_{50\%}} = \frac{d_{50\%}}{d_{15.9\%}} = \left(\frac{d_{84.1\%}}{d_{15.9\%}}\right)^{\frac{1}{2}} \quad (7)$$

In addition to the calculation of MMD and GSD, the percentages of PM_{10} and PM_5 by volume were also calculated from the cumulative PSD curves (Hinds, 1999; Zhang, 2005). PM_5 represents the respirable size fraction based on the suggested definition by Donham et al. (1989). The range of diameters containing 95% of particles with lognormal distribution was calculated using equation 8. The 95% confidence intervals (CIs) for MMD, GSD, PM_5 and PM_{10} were calculated using equations 9 to 12:

$$\exp[\ln \mathrm{MMD} \pm 2 \ln \delta_g] \quad (8)$$

$$95\%\ \mathrm{CI\ for\ MMD} = \overline{\mathrm{MMD}} \pm t\delta_{\mathrm{MMD}} \quad (9)$$

$$95\%\ \mathrm{CI\ for\ GSD} = \overline{\mathrm{GSD}} \pm t\delta_{\mathrm{GSD}} \quad (10)$$

$$95\%\ \mathrm{CI\ for\ PM_5} = \overline{\mathrm{PM}_5} \pm t\delta_{\mathrm{PM5}} \quad (11)$$

$$95\%\ \mathrm{CI\ for\ PM_{10}} = \overline{\mathrm{PM}_{10}} \pm t\delta_{\mathrm{PM10}} \quad (12)$$

where $\overline{\mathrm{MMD}}$, $\overline{\mathrm{GSD}}$, $\overline{\mathrm{PM}_5}$, and $\overline{\mathrm{PM}_{10}}$ are the respective mean values, and t is the t-test value at a p-value of 0.05.

Analysis of variance (ANOVA) was used to test the significance of the differences among the means of particle size statistics at daytime vs. nighttime and at elevations of 0.8 vs. 1.6 m. ANOVA was also applied to determine if there were significant day-to-day variations in the particle size statistics.

Results and Discussion

Ventilation Rates

During the winter sampling, all exhaust fans in the building were off and only two of the pit fans were on. The 24 h average ventilation rate (Q_b) for the building ranged from 0.76 to 3.73 $m^3\ s^{-1}$. The actual 24 h daytime (6:00 to 18:00 h), and nighttime (18:00 to 6:00 h) average ventilation rates in December are shown in figure 5. The ventilation rate during daytime and nighttime did not vary significantly, with values ranging from 0.75 to 3.71 for daytime and from 0.77 to 3.85 for nighttime. In six out of ten days, the daytime average ventilation rates were higher than the nighttime averages by as much as 31%. The ventilation rate was nearly constant during the first five days of sampling and started to increase during the following four days, with the ventilation rate peaking on December 14. The corresponding daily averages of outdoor temperature (T_o) are also shown in figure 5. The daily average T_o ranged from -9.7° to 13.2°C. In general, an increase in T_o is accompanied by an increase in ventilation rate to maintain an approximately constant temperature of 25°C inside the building.

The daily, daytime, and nighttime averages of ventilation rates measured in June are presented in figure 6. The daily average ventilation rates ranged from 23.21 to 46.03 $m^3\ s^{-1}$; the daytime and nighttime averages ranged from 14.71 to 44.27 $m^3\ s^{-1}$ and from 31.71 to 47.79 $m^3\ s^{-1}$, respectively. Unlike the winter measurements, the daytime and nighttime ventilation rates were significantly different ($p < 0.05$) from each other; the daily daytime averages were consistently

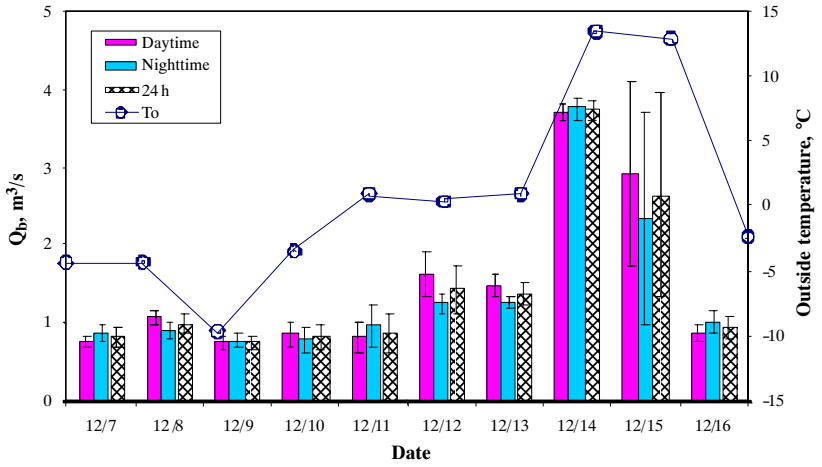

Figure 5. Daytime, nighttime, and 24 h averages of ventilation rates, and the average daily outside temperature in December (error bars indicate standard deviations).

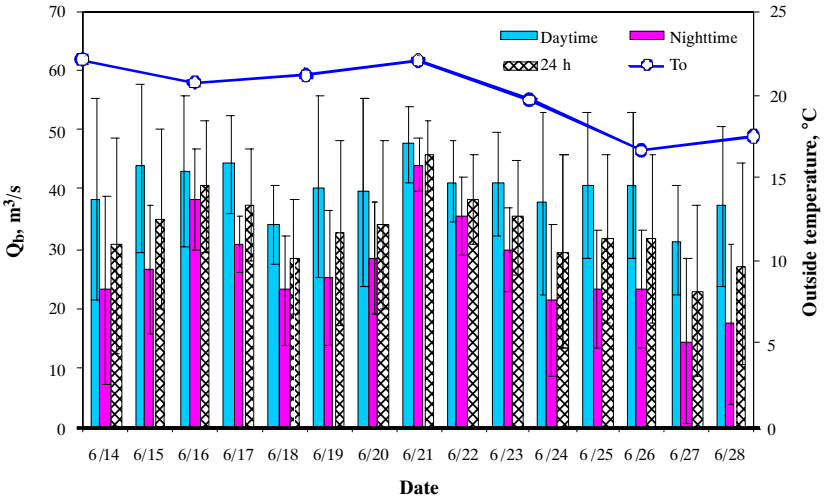

Figure 6. Daytime, nighttime, and 24 h averages of ventilation rates, and the average daily outside temperature in June (error bars indicate standard deviations).

higher than the measured nighttime ventilation rates by as much as 54%. The outside temperature also fluctuated throughout the measurement period, with the daily averages ranging from 16.5˚ to 22.14˚C.

Comparison of PSD as Measured by the Coulter Counter and Horiba LA-300

The PSD of PM collected from a swine building was analyzed using both Coulter Counter and Horiba LA-300 analyzers. The PM samples collected in December were analyzed with the Coulter Counter, while the samples collected in June were analyzed with the Horiba LA-300. In order to compare the results of the two analyzers, 30 of the collected samples in June were analyzed using both instruments. In choosing the filter samples to be analyzed, only those with uniform particle loading throughout each filter were selected. Each of these 30 filter samples was cut in half: half was sent to Texas A&M for Coulter Counter analysis, while the other half was used for Horiba LA-300 analysis.

A paired t-test analysis was applied to determine if the differences in the MMD, GSD, %PM_5, and %PM_{10} measured with the Coulter Counter and Horiba LA-300 analyzers were significant at the 5% level. Results showed that the aforementioned values between the two analyzers were significantly different. Table 1 shows the PSD statistics for the Coulter Counter and Horiba LA-300 measurements. The MMD and GSD of the PSD measured with the Horiba LA-300 were higher by about 42% and 20%, respectively, than those measured with the Coulter Counter. The percentage by volume of PM_5 measured with the Coulter Counter was significantly lower than with the Horiba (0.63% vs. 3.3%), and the percentage by volume of PM_{10} was also significantly lower, by 78%, with the Coulter Counter than with the Horiba (4.84% vs. 8.62%).

The lower percentage of PM_5 and PM_{10} could be attributed to the aperture that was used in the Coulter Counter analysis. The aperture of 100 μm only allowed particles with diameters of 2.95 to 60 μm to be measured. In the Horiba analysis, particles smaller than 3 μm constituted about 2%, which was not accounted for in the Coulter Counter measurements. Similarly, the percentage of particles larger than 60 μm, which was also not accounted for in the Coulter Counter measurements, was about 16% on average and was as high as 48%. Also shown in table 1 are the particle statistics when only the size fractions between 3 and 60 μm

Table 1. Comparison of the PSD statistics measured by the Coulter Counter and Horiba LA-300 analyzers. The presented diameters are the aerodynamic diameters. Thirty samples each for Coulter Counter and Horiba were used in the analysis.

	Coulter Counter		Horiba LA-300[a]		Horiba LA-300[b]	
Parameter	Mean	95% CI	Mean	95% CI	Mean	95% CI
MMD (μm)	22.63	(21.67, 23.59)	32.23	(31.27, 33.20)	27.31	(26.44, 28.18)
GSD	1.58	(1.55, 1.61)	1.89	(1.86, 1.93)	1.92	(1.87, 1.96)
PM_5 (%)	0.61	(0.46, 0.75)	3.30	(3.15, 3.44)	2.21	(1.78, 2.65)
PM_{10} (%)	4.84	(4.37, 5.30)	8.62	(8.15, 9.09)	7.31	(6.73, 7.89)

[a] Results when all size fractions were used in the comparison.
[b] Results when only size fractions between approximately 3 μm and 60 μm were used in the comparison.

for the Horiba LA-300 were included in the analysis. There was a significant decrease in the MMD because of the removal of particles larger than 60 μm in the analysis, and the PM_5 and PM_{10} decreased due to the removal of particles smaller than 3 μm. Paired t-tests also showed that the MMD, GSD, $\%PM_5$, and $\%PM_{10}$ measured with the Coulter Counter and Horiba LA-300 analyzers were significantly different at the 5% level.

Shown in figure 7 is the cumulative mass or volumetric fraction of the particle population based upon MMD and GSD values measured with both the Coulter Counter and the Horiba LA-300. The curves were constructed using equation 6, and the MMD and GSD for each PSD are presented in table 1. The MMD values of the two curves differ by 9.6 μm. For the Coulter Counter, 95% of the particles were between 9 and 56.5 μm in diameter; for the Horiba LA-300, 95% of the particles were between 9 and 115.5 μm. However, it should be noted that the size measurement ranges of the two analyzers differed: the Coulter Counter measured particles from 3 to 60 μm, and the Horiba LA-300 measured particles from 0.1 to 600 μm. For the Horiba LA-300, an upper size range of 56.5 μm constituted only about 80% of the total particle population by volume. Thus, for particle sizes up to 56.5 μm, there was a discrepancy of 15% in the measurements using the two analyzers. Consequently, the PSDs of the samples collected in December, which were obtained using the Coulter Counter, cannot be directly compared with the resulting PSDs of the samples collected in June, which were analyzed using the Horiba LA-300.

Temporal Variation in Particle Size Distribution

A total of 144 and 180 samples collected indoors in December and June, respectively, were analyzed for PSD. In order to determine the possible variation in PSD during daytime and nighttime sampling, half of the samples were from daytime and the other half were chosen from the nighttime samples collected over several days (four days in December and five days in June). As indicated previously, all of the samples collected in December were analyzed with the Coulter Counter, while the Horiba LA-300 was used exclusively for the samples collected in June.

The analysis of the filter samples showed that about 10% of the swine PM was less than 12 μm in aerodynamic diameter by volume, indicating that more than 90% of the swine PM was greater than the regulated particle sizes of PM_{10} and $PM_{2.5}$. Ninety percent of the particles by volume were less than 69 μm in diameter when the Horiba LA-300 was used; with the Coulter Counter, 90% of the particles were

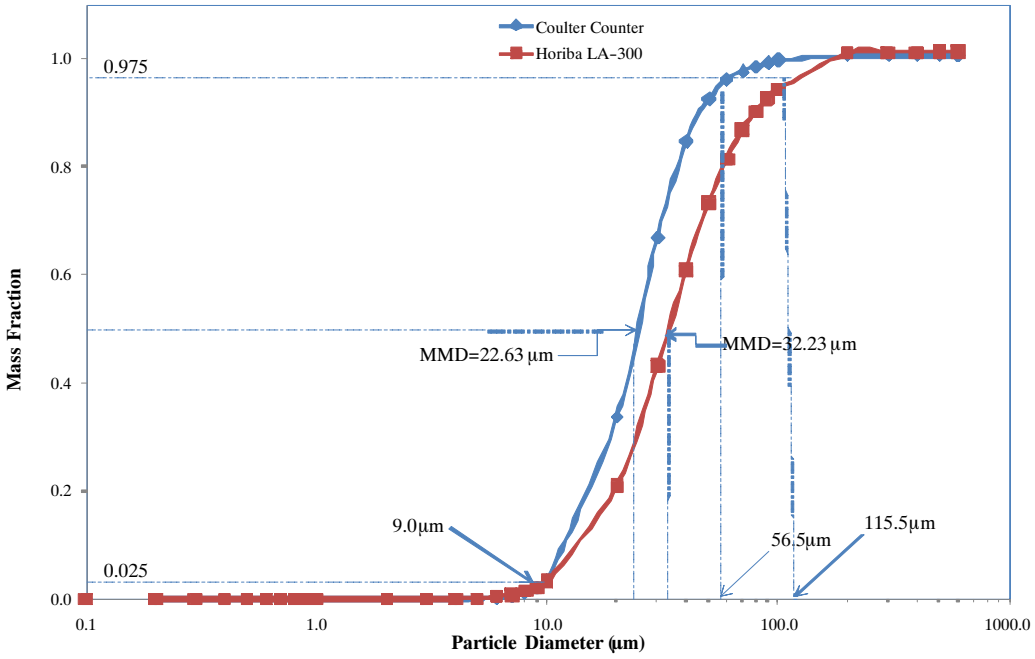

Figure 7. Comparison of the cumulative mass fraction of a particle population with an average MMD of 22.63 μm and a GSD of 1.58 for the Coulter Counter and an average MMD of 32.23 μm and a GSD of 1.89 for the Horiba LA-300. The 95% CI for the MMD and GSD values used in generating these curves are presented in table 1.

Table 2. Swine PM size data by day in December. PM samples were analyzed with the Coulter Counter analyzer.[a]

		December 10		December 13		December 15		December 16	
Parameter[b]		AM	PM	AM	PM	AM	PM	AM	PM
MMD (μm)	Mean	20.33	24.72	19.90	20.94	20.51	21.19	20.77	20.37
	SD	1.01	3.59	2.52	2.90	2.02	2.40	1.14	1.40
	Min	18.44	21.12	13.72	12.85	14.23	14.23	19.22	17.40
	Max	22.02	34.98	22.16	24.19	23.13	24.42	23.46	22.73
GSD	Mean	1.50	1.42	1.50	1.49	1.51	1.50	1.51	1.49
	SD	0.05	0.09	0.04	0.03	0.06	0.05	0.04	0.05
	Min	1.42	1.09	1.44	1.43	1.42	1.42	1.46	1.43
	Max	1.58	1.51	1.56	1.54	1.59	1.59	1.58	1.58
PM_5 (%)	Mean	0.71	0.53	0.85	0.98	0.76	0.78	0.80	0.83
	SD	0.13	0.13	0.14	0.21	0.15	0.14	0.10	0.13
	Min	0.47	0.33	0.60	0.59	0.51	0.51	0.59	0.64
	Max	0.93	0.78	1.18	1.35	1.00	1.00	0.98	1.09
PM_{10} (%)	Mean	7.10	4.25	7.35	6.72	7.15	6.66	7.44	7.62
	SD	1.09	0.93	1.05	0.95	1.17	1.37	0.92	1.40
	Min	5.06	2.77	5.50	5.28	5.43	4.74	6.07	5.99
	Max	9.16	5.69	9.09	8.68	8.99	8.99	8.89	10.70

[a] AM = daytime; PM = nighttime.
[b] Overall means: MMD = 21.10 μm, GSD = 1.49, PM_5 = 0.78%, and PM_{10} = 6.79%.

Table 3. Swine PM size data by day in June. PM samples were analyzed with the Horiba LA-300 analyzer.[a]

		June 15		June 18		June 21		June 24		June 27	
Parameter[b]		AM	PM	AM	PM	AM	PM	AM	PM	AM	PM
MMD (μm)	Mean	32.14	28.60	31.05	31.12	37.32	32.06	32.92	31.81	30.27	28.19
	SD	6.71	4.52	3.76	2.17	10.68	7.85	3.73	4.87	3.61	2.59
	Min	24.26	19.06	27.42	26.91	15.39	25.54	27.64	24.59	24.73	23.40
	Max	50.67	39.49	41.43	35.00	60.18	55.69	39.58	46.68	36.01	32.13
GSD	Mean	2.02	2.02	1.95	1.76	1.94	1.77	1.84	1.80	1.78	1.74
	SD	0.18	0.41	0.20	0.08	0.42	0.15	0.13	0.15	0.19	0.13
	Min	1.71	1.46	1.74	1.57	1.27	1.42	1.59	1.52	1.57	1.51
	Max	2.42	3.21	2.28	1.88	3.26	2.09	2.10	2.05	2.29	1.91
PM_5 (%)	Mean	2.69	2.38	2.79	2.50	2.86	2.90	3.00	3.47	3.10	3.69
	SD	0.51	0.87	0.67	0.88	0.58	0.61	0.44	0.66	0.75	1.30
	Min	1.20	0.22	1.29	0.08	1.65	1.40	2.39	2.72	1.20	2.41
	Max	3.31	3.88	3.87	3.64	4.15	3.92	3.99	4.86	4.39	8.14
PM_{10} (%)	Mean	8.30	7.89	7.49	6.31	7.23	6.49	7.92	8.75	8.54	9.75
	SD	1.52	2.03	1.48	1.55	1.61	1.19	1.28	1.22	2.09	2.10
	Min	4.71	3.37	3.79	2.41	4.62	3.92	5.39	7.25	3.64	7.59
	Max	11.30	11.95	10.07	9.69	11.06	8.47	9.85	11.40	11.67	15.63

[a] AM = daytime; PM = nighttime.
[b] Overall means: MMD = 31.55 μm, GSD = 1.86, PM_5 = 2.94%, and PM_{10} = 7.87%.

less than 34 μm in diameter. Other swine PM particle size statistics are given by sampling day in table 2 for December and in table 3 for June. The average percentage of PM_5 was about 3% for the Horiba LA-300 and less than 1% for the Coulter Counter. About 8% of the particles by volume were PM_{10}.

The average MMD for all sampling days and sampling locations was 21.10 μm in December, which was about 50% lower than the average MMD of 31.55 μm in June. Lee at al. (2008) conducted a similar study in eight swine farms in Illinois. For PM sized with a Horiba LA-300, the reported MMDs ranged from 19.2 to 24.5 μm and the GSDs ranged from 2.2 to 3.4. They also used a Coulter Counter in PSD analysis, and the reported MMDs ranging from 9.5 to 16.5 μm and the GSDs ranged from 1.7 to 2.4. In the current study, the individual MMD means varied from 19.90 to 24.70 μm in December and from 28.19 to 37.32 in June. The GSDs in December and June were also different, with the mean GSD of 1.86 in June higher than the mean GSD of 1.49 in December by about 25%. The daily GSD varied from 1.42 to 1.51 in December and from 1.74 to 2.02 in June. Similarly, the percentages of PM_5 and PM_{10} in June were also higher than in December by 376% and 16%, respectively. These differences in particle statistics could be attributed to the different ranges of the PSD analyzers that were used in the analyses, as discussed in the previous section.

ANOVA was applied to determine if there was a significant day-to-day variation in the particle statistics presented in tables 2 and 3. Some of the major factors that could cause the day-to-day variation in PSD are the differences in the activities of the workers and animals in the building, animal age, and the varying ventilation rates shown in figures 5 and 6. In general, the data satisfied the normality and equality of variance assumptions of ANOVA. Normality was determined by looking at the normal probability plot, while the equality of variance assumption was tested by

Table 4. The 95% confidence limits of swine PM measured indoors.

	December 2005		June 2006	
Parameter	Lower Limit	Upper Limit	Lower Limit	Upper Limit
MMD (μm)	20.33	21.87	30.79	32.21
GSD	1.46	1.52	1.83	1.89
PM_5 (%)	0.68	0.88	2.85	3.04
PM_{10} (%)	6.50	7.07	7.63	8.15

applying Levene's test for equality of variances. In general, the day-to-day variation in MMD, GSD, %PM_5, and %PM_{10} were significant, suggesting that for accurate estimate of PSD in animal buildings, more measurements should be conducted. The 95% confidence limits for the various particle statistics are presented in table 4.

A paired t-statistic analysis, which was done to evaluate if the difference between the particle statistics at daytime (AM) and nighttime (PM) was significant at the 5% level, revealed mixed results. For both December and June, the MMDs and GSDs between AM and PM sampling were significantly different, while the %PM_5 and %PM_{10} were not. In December, the MMDs at AM were, in general, lower than the MMDs at PM, which contradicted the result in June. The GSDs at AM, on the other hand, were higher than the GSDs at PM in both December and June.

Spatial Variation of Particle Size Distribution

The average values of particle size statistics are given per sampling location in table 5. The MMD averaged over all four days in December and five days in June and over all sampling locations was 21.10 μm in December and 31.55 μm in June. The individual means per sampling location varied from 18.34 to 23.35 μm in December and from 27.09 to 39.32 μm in June. The average GSDs were 1.49 and 1.56 in December and June, respectively, ranging from 1.41 to 1.56 in December and from 1.74 to 2 in June. In the sampling locations listed in table 5, the Roman numeral refers to the cross-section of the building where the samples were collected; sampling locations 1, 3, and 5 were located at 1.6 m above the floor, while locations 6, 8, and 10 were at an elevation of 0.8 m. Results of ANOVA showed that, in general, the MMD, GSD, %PM_5, and %PM_{10} at an elevation of 0.8 m were not significantly different from those obtained at 1.6 m.

The spatial distributions of MMD, GSD, %PM_5, and %PM_{10} in December are shown in figure 8. Although the highest MMD and GSD were obtained near the endwall inlet and exhaust fans of the building, the gradients were small. It should be noted that the exhaust fans were located about 7 m away from where the samples were obtained near the outlet. High MMD and GSD values near the endwall inlet and exhaust side are expected, since the pigs that were located in the pens near these locations were bigger and could have contributed more to PM production. The spatial distributions of %PM_5 and %PM_{10}, shown in figures 8c and 8d, respectively, appear to be uniform, with the percent concentration varying by less than 1%. The spatial distributions of the mass concentrations of PM_5 and PM_{10} are plotted in figure 9. The mass concentrations of PM_5 ranged from 0.007 to 0.029 mg m^{-3}, while PM_{10} ranged from 0.073 to 0.232 mg m^{-3}. Even if the gradient was small, the spatial distributions of the mass concentrations appear to follow the distribution of MMD and GSD in figures 8a and 8b, respectively.

Shown in figure 10 are the spatial distributions of MMD, GSD, %PM_5, and %PM_{10} in June. When the building was tunnel-ventilated, the MMD and GSD values, in general, tended to decrease toward the outlet, which was expected, since the range of particle sizes remaining airborne decreased as larger particles settled out. The %PM_5 and %PM_{10}, however, followed the spatial distribution of the TSP mass concentration, in which the percent concentration increased toward the outlet side of the building. Similarly, the spatial distributions of the mass concentrations of PM_5 and PM_{10},

Table 5. Average values of particle statistics.

Sampling Location[a]	December[b]				June[c]			
	MMD (μm)	GSD	PM_5 (%)	PM_{10} (%)	MMD (μm)	GSD	PM_5 (%)	PM_{10} (%)
I-1	20.85	1.46	0.64	6.42	35.51	1.93	2.32	5.67
I-3	21.82	1.56	0.93	7.37	36.06	2.00	2.79	7.03
I-5	20.46	1.49	0.87	7.81	34.21	1.83	2.64	7.14
I-6	21.71	1.50	0.74	6.32	39.32	1.80	3.01	6.90
I-8	22.16	1.55	0.87	6.92	32.73	1.86	2.85	6.92
I-10	20.88	1.52	0.92	7.80	36.30	1.92	2.80	7.14
III-1	18.34	1.43	0.71	7.77	27.65	1.80	3.06	8.73
III-3	21.14	1.52	0.75	6.81	32.80	1.91	2.80	7.57
III-5	19.38	1.48	0.84	8.29	28.96	1.80	2.93	8.13
III-6	20.50	1.47	0.74	6.45	30.47	1.98	2.91	8.00
III-8	21.34	1.52	0.85	7.09	32.62	1.95	2.90	7.53
III-10	21.83	1.51	0.77	6.23	28.50	1.77	3.13	8.63
V-1	20.48	1.44	0.76	6.43	28.67	1.74	2.76	8.23
V-3	23.01	1.51	0.76	5.67	30.46	1.88	3.27	8.87
V-5	19.83	1.45	0.78	7.49	27.09	1.93	3.44	8.83
V-6	21.45	1.41	0.69	5.83	29.91	1.81	2.80	8.20
V-8	23.35	1.53	0.75	5.56	30.15	1.87	3.33	9.10
V-10	21.26	1.45	0.68	6.01	29.45	1.77	2.92	8.01
Mean	21.10	1.49	0.78	6.79	31.55	1.56	2.94	7.87

[a] Selected sampling locations depicted in figure 2.
[b] Each value represents the average of eight replicates.
[c] Each value represents the average of ten replicates.

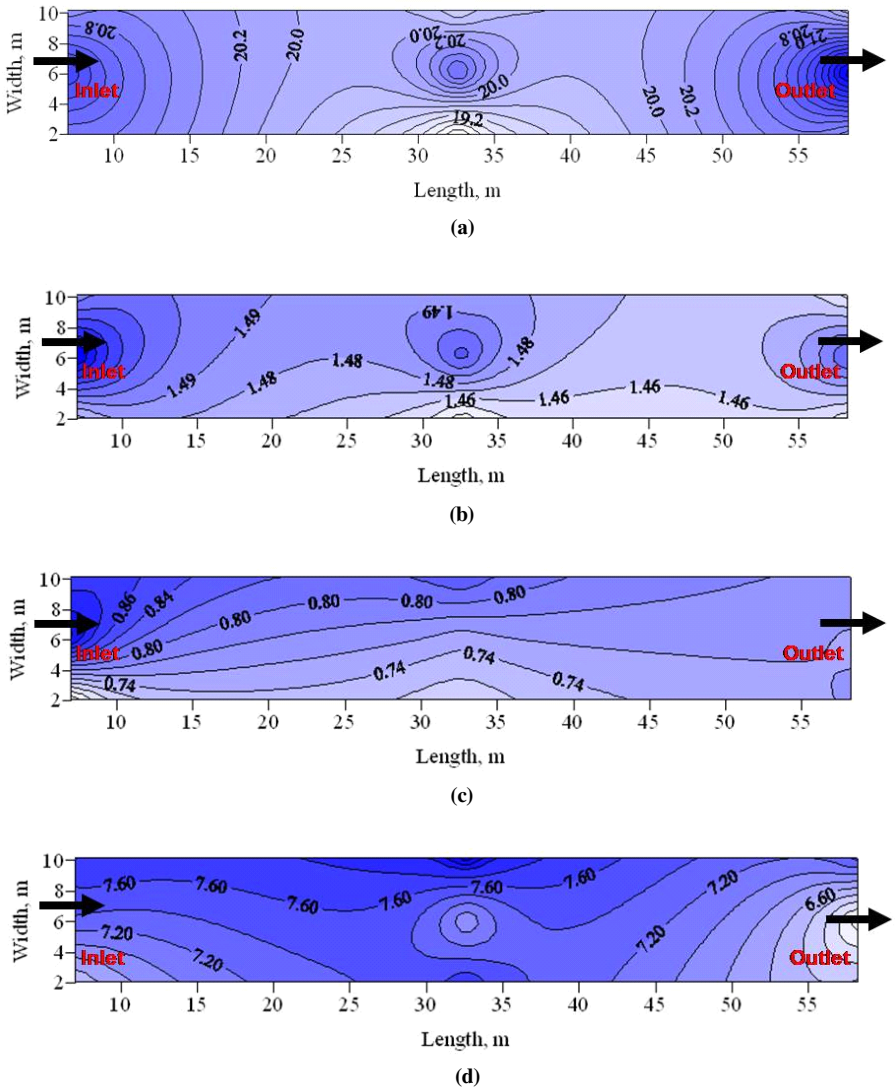

Figure 8. Spatial distribution of the average (a) MMD (µm), (b) GSD, (c) %PM_5, and (d) % PM_{10} in December. All values were taken at 1.6 m from the floor. Data were plotted using Surfer version 7, which uses the weighted average interpolation algorithm.

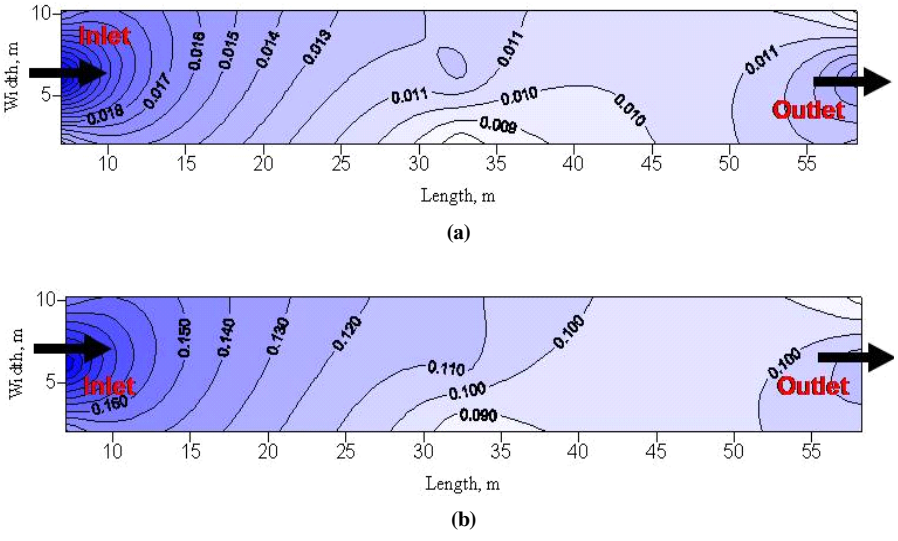

Figure 9. Spatial distribution of the average mass concentration (mg m^{-3}) of (a) PM_5 and (b) PM_{10} in December. All values were taken at 1.6 m from the floor. Data were plotted using Surfer version 7, which uses the weighted average interpolation algorithm.

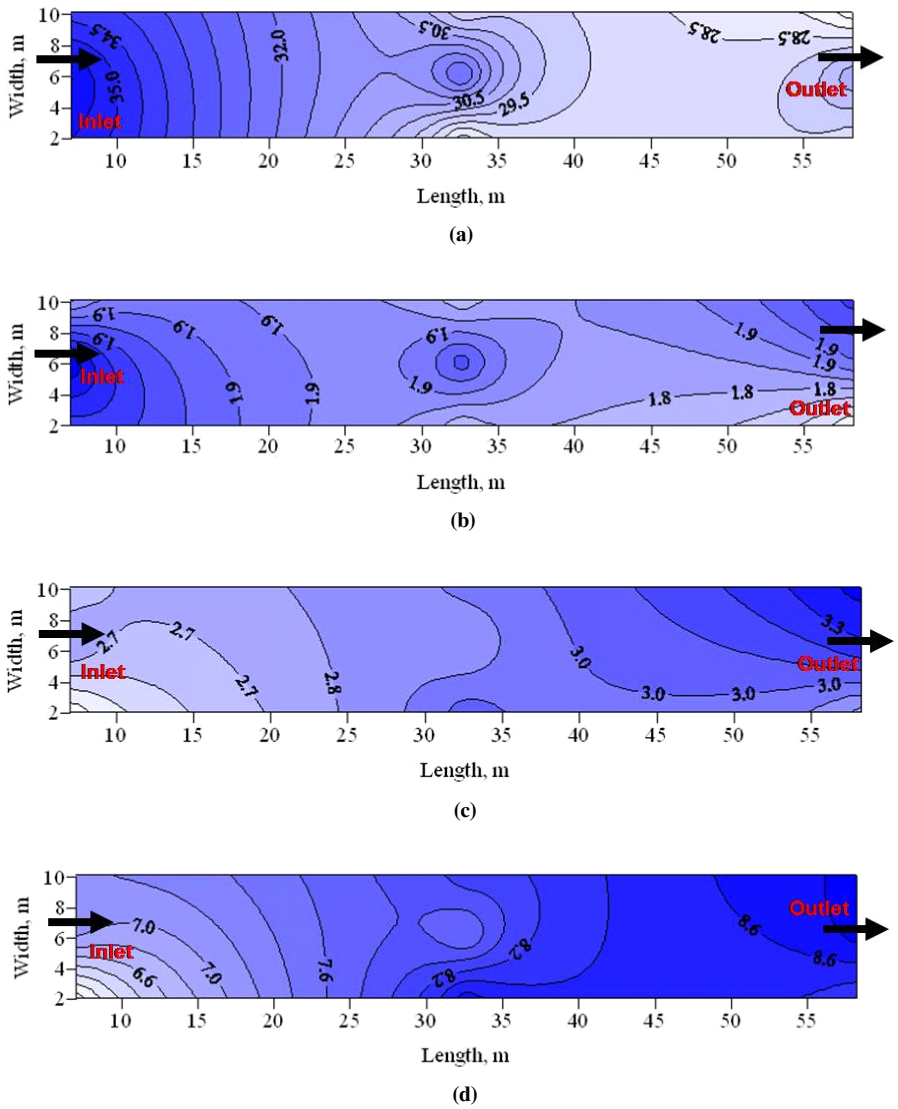

Figure 10. Spatial distribution of the average (a) MMD (μm), (b) GSD, (c) %PM_5, and (d) % PM_{10} in June. All values were taken at 1.6 m from the floor. Data were plotted using Surfer version 7, which uses the weighted average interpolation algorithm.

shown in figure 11, followed the spatial distribution of the TSP mass concentration. The equivalent mass concentrations of PM_5 ranged from 0.006 to 0.046 mg m^{-3}, and PM_{10} mass concentrations ranged from 0.014 to 0.125 mg m^{-3}. Thus, in a tunnel-ventilated building, large particles settled out, but smaller particles (<10 μm) accumulated as the air moved from one end to the opposite end of the building.

The PSD of swine PM leaving the building was also analyzed by collecting samples upstream of the exhaust fans. The total number of samples that were used in the analysis was 52, collected during daytime and nighttime. ANOVA results revealed that the particle statistics presented in table 6 did not vary significantly between daytime and nighttime. Shown in table 7 is a comparison of the particle statistics indoors and at the exhaust. Compared to the average MMD indoors, the average MMD of PM leaving the building was significantly lower by about 18% (26.79 vs. 31.55 μm), while the GSDs and %PM_5 were about equal (1.84 vs. 1.86 for GSD and 2.94 vs. 2.97 for %PM_5). The %PM_{10} leaving the building was significantly higher by about 19% compared to the average value indoors (9.36% vs. 7.87%). Lower MMD but higher %PM_{10} near the exhaust suggests that the percentage of particles larger than 10 μm remaining in the air decreased due to settling, while PM_{10} continued to accumulate.

Figure 12 shows the cumulative curves by volume of swine PM obtained indoors and near the exhaust. These curves were obtained by using the corresponding MMD and GSD values and applying equation 6. The MMDs and % PM_{10} between indoors and at the exhaust were significantly different at the 5% level, while the GSDs and %PM5 did not vary significantly. Since the GSD values of the exhaust and indoors were almost the same, the slopes of the curves are similar, and the MMD for indoors shifted to the right by about 5 μm.

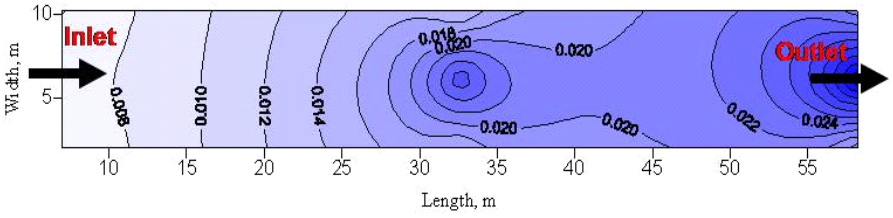

(a)

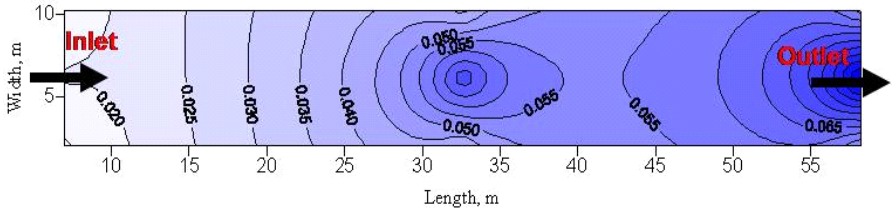

(b)

Figure 11. Spatial distribution of the average mass concentration (mg m^{-3}) of (a) PM_5 and (b) PM_{10} in June. All values were taken at 1.6 m from the floor. Data were plotted using Surfer version 7, which uses the weighted average interpolation algorithm.

Table 6. The 95% confidence limits of the particle size of swine PM leaving the building at daytime (AM) and nighttime (PM).

Parameter	AM			PM			Overall Average
	Average	Lower Limit	Upper Limit	Average	Lower Limit	Upper Limit	
MMD (μm)	26.10	24.49	27.77	27.48	25.92	29.20	26.79
GSD	1.86	1.76	1.94	1.83	1.75	1.93	1.84
PM_5 (%)	2.94	2.51	3.39	3.00	2.50	3.38	2.97
PM_{10} (%)	9.55	8.66	10.48	9.16	8.10	9.92	9.36

Table 7. The 95% confidence limits of the particle size of swine PM indoors and at the exhaust.

Parameter	Indoors			Exhaust		
	Average	Lower Limit	Upper Limit	Average	Lower Limit	Upper Limit
MMD (μm)	31.55	29.60	33.50	26.79	24.84	28.74
GSD	1.86	1.77	1.95	1.84	1.76	1.93
PM_5 (%)	2.94	2.58	3.30	2.97	2.61	3.33
PM_{10} (%)	7.87	7.04	8.69	9.36	8.53	10.18

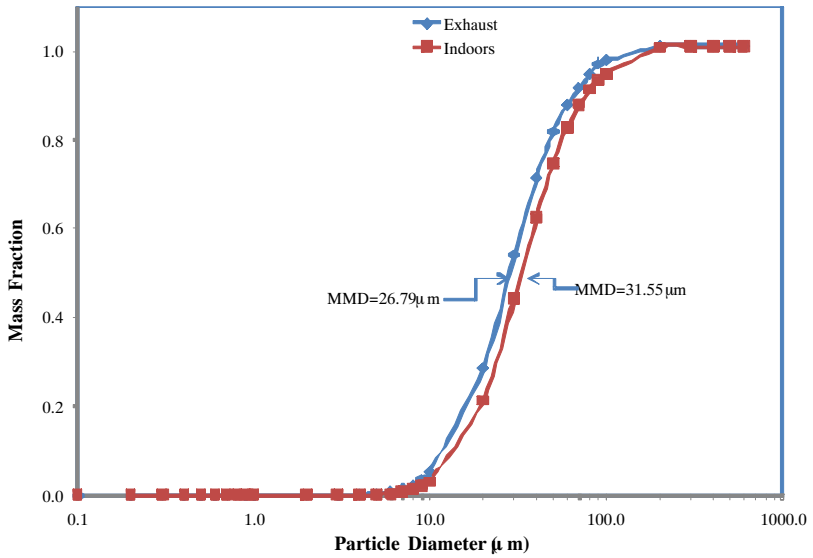

Figure 12. Comparison of the cumulative volumetric fraction of swine PM measured at the exhaust (with an MMD of 26.79 μm and GSD of 1.84) and indoors (with an MMD of 31.55 μm and GSD of 1.86).

CONCLUSION

The PSDs indoors and upstream of the exhaust fans of a commercial swine building were measured and compared. All measurements were done in December 2005 and June 2006. The following conclusions were drawn from this study:

- The MMD and GSD of swine PM were significantly affected by the range of measurements of the analyzer. The MMD and GSD measured with the Horiba LA-300 were higher by about 42% and 20%, respectively, than those measured with the Coulter Counter.
- There was no significant vertical variation in the MMD and GSD of swine PM measured at elevations of 0.8 and 1.6 m.
- During winter, higher MMD and GSD were observed over the pens that held bigger and more active pigs. In summer, the MMD and GSD tended to decrease from the endwall inlet toward the outlet due to settling of large particles. On the other hand, the PM_5 and PM_{10} concentrations increased toward the outlet as more PM accumulated.
- The spatial distributions of PM_5 and PM_{10} appeared to be uniform during winter. In summer, the PM_5 and PM_{10} followed the spatial distribution of the TSP mass concentration, which tended to increase toward the outlet as more PM accumulated.
- The percentage of PM_{10} leaving the building was only 10% of the total particle concentration. This value was close to the average percentage indoors. In terms of mass, the concentration of PM_{10} leaving the building ranged from 0.02 to 0.15 mg m^{-3}.
- The average MMD of swine PM at the exhaust was lower than the MMD indoors by about 14% (26.84 vs. 31.55 μm), while the GSD values were about the same (1.85 vs. 1.86).

ACKNOWLEDGEMENTS

We are grateful to Dr. Bryan Shaw's research group at Texas A&M, particularly John Wanjura, for helping with the PSD analysis. The authors are also thankful to Jingwei Su, Research Engineer at the Department of Biological and Agricultural Engineering, UIUC, for helping with the data collection.

REFERENCES

Beckman Coulter. 2000. *Coulter Counter Multisizer 3 User's Manual.* Hialeah, Fla.: Beckman Coulter, Inc.

Buser, M. D. 2004. Errors associated with particulate matter measurements on rural sources: Appropriate basis for regulating cotton gins. PhD diss. College Station, Tex.: Texas A&M University, Department of Biological and Agricultural Engineering.

Capareda, S. G., C. B. Parnell, B. W Shaw, and J. D. Wanjura. 2005. Particle size distribution analyses of agricultural dusts and report of true PM_{10} concentrations. ASABE Paper No. 054044. St. Joseph, Mich.: ASABE.

Cooper, D. W. 2001. Methods of size distribution data analysis and presentation. In *Aerosol Measurement: Principles, Techniques, and Applications*, 667-701. P. A.Baron and K. Willeke, eds. New York, N.Y.: John Wiley and Sons.

Donham, K., P. Haglind, Y. Peterson, R. Rylander, and L. Belin. 1989. Environmental and health studies of workers in Swedish swine confinement buildings. *British J. Ind. Med.* 46(1): 31-37.

Ellen, H. H., R. W. Bottcher, E. von Wachenfelt, and H. Takai. 2000. Dust levels and control methods in poultry houses. *J. Agric. Safety and Health* 6(4): 275-283.

EPA. 2000. List of designated promulgated test methods: Methods for measurement of filterable PM_{10} and $PM_{2.5}$ and measurement of condensable PM emissions from stationary sources. Research Triangle Park, N.C.: U.S. Environmental Protection Agency.

Gay, S. W., C. J. Clanton, D. R. Schmidt, K. A. Janni, L. D. Jacobson, and S. Weisberg. 2003. Odor, total reduced sulfur, and ammonia emissions from animal housing facilities and manure storage units in Minnesota. *Applied Eng. in Agric.* 19(3): 347-360.

Heber, A. J., J.-Q. Ni, B. L. Haymore, R. K. Duggirla, and K. M. Keener. 2001. Air quality and emission measurement methodology at swine finishing buildings. *Trans. ASAE* 44(6): 765-1178.

Hinds, W. C. 1999. *Aerosol Technology: Properties, Behavior, and Measurement of Airborne Particles.* New York, N.Y.: John Wiley and Sons.

Horiba. 2001. *Laser Scattering Particle Size Analyzer LA-300 User's Manual.* Kyoto, Japan: Horiba, Ltd.

Jacobson, L. D., A. J. Heber, Y. Zhang, J. Koziel, J. M. Sweeten, D. S. Bundy, and R. W. Bottcher. 2003. Aerial pollutant emissions from pig and poultry confinement buildings in the United States. In *Proc. Intl. Symp. Gaseous and Odor Emissions from Animal Production Facilities*, 194-202. Horsens, Denmark: CIGR.

Jerez, S. B., Y. Zhang, J. W. McClure, A. J. Heber, J.-Q. Ni, J. A. Koziel, S. J. Hoff, and L. D. Jacobson. 2005. Aerial pollutant concentration and emission rate measurements from a swine farrowing building in Illinois. In *Proc A&WMA 98th Annual Conf. and Exhibition.* Paper No. 1026. Pittsburgh, Pa.: Air and Waste Management Association.

Jerez, S. B., Y. Zhang, J. McClure, L. Jacobson, A. Heber, S. Hoff, J. Koziel, and D. Beasley. 2006. Comparison of measured total suspended particulate matter concentration using tapered element oscillating microbalance and a TSP sampler. *J. A&WMA* 56(3): 261-270.

Lee, J., Y. Zhang, X. Wang, X. Yang, J. Su, B. Faulkner, B. W. Shaw, and G. L. Riskowski. 2008. Measurement of particle size distributions in swine buildings. In *Proc. Intl. Symp. Livestock Environment VIII*, 95-100. St. Joseph, Mich.: ASABE.

Lines, R. W. 1991. The electrical sensing zone method (the Coulter principle). In *Proc. 25th Anniversary Conf. Organized by the Particle Characterization Group of the Analytical Division of the Royal Spciety of Chemistry*, 351-373. N. G. Stanley-Wood and R. W. Lines, eds. Cambridge, U.K.: Royal Society of Chemistry.

NAS. 2003. Air emissions from animal feeding operations: Current knowledge, future needs, 2: 50-56. Washington, D.C.: National Academy of Sciences.

Ni, J.-Q., A. J. Heber, T. T. Lim, C. A. Diehl, R. K. Duggirala, B. L. Haymore, and A. L. Sutton. 2000. Ammonia emissions from a large mechanically ventilated swine building during warm weather. *J. Environ. Qual.* 29(3): 751-758.

Ni, J.-Q., A. J. Heber, C. A. Diehl, T. T. Lim, R. K. Duggirala, and B. L. Haymore. 2002. Summertime concentrations and emissions of hydrogen sulfide at a mechanically ventilated swine finishing building. *Trans. ASAE* 45(1): 193-199.

O'Shaughnessy, P. T., C. Achutan, and A. W. Karsten. 2002. Temporal variation of indoor air quality in an enclosed swine confinement building. *J. Agric. Safety and Health* 8(4): 349-364.

Predicala, B. Z., and R. G. Maghirang. 2002. Measurement of particulate matter emission rates from mechanically ventilated swine barns. *Trans. ASAE* 47(2): 557-565.

Predicala, B. Z., R. G. Maghirang, S. B. Jerez, J. E. Urban, and R. D. Goodband. 2001. Dust and bioaerosol concentrations in two swine-finishing buildings in Kansas. *Trans. ASAE* 44(5): 1291-1298.

Redwine, J. S., and R. E. Lacey. 2001. Concentration and emission of ammonia and particulate matter in tunnel-ventilated broiler houses under summer conditions in Texas. ASAE Paper No. 014095. St. Joseph, Mich.: ASAE.
Schneider, F. E., T. Engelhardt, and P. W. Wieser. 2001. Characterization of aerosol particles from animal husbandry with single-particle analytic techniques. ASAE Paper No. 014010. St. Joseph, Mich.: ASAE.
Sweeten, J. M., C. B. Parnell, B. W. Shaw, and B. W. Auvermann. 1998. Particle size distribution of cattle feedlot dust emission. *Trans. ASAE* 41(5): 1477-1481.
Tompkins, H. 2006. *A User's Guide to Ellipsometry.* New York, N.Y.: Academic Press.
Vinzents, P. S. 1994. Mass distribution of inhalable aerosols in swine buildings. *American Ind. Hyg. Assoc. J.* 55(10): 977-980.
Zhang, Y. 2005. *Indoor Air Quality Engineering.* Boca Raton, Fla.: CRC Press.
Zhang, Y., X. Wang, G. L. Riskowski, and L. L. Christianson. 2001. Quantifying ventilation effectiveness for air quality control. *Trans. ASAE* 44(2): 385-390.